

MICHIGAN STATE UNIVERSITY

CYCLOTRON LABORATORY

The Effect of Space Charge on Beams Extracted
from the RTECR Ion Source

Z.Q. Xie and T.A. Antaya
National Superconducting Cyclotron Laboratory
Michigan State University
E. Lansing, MI 48824-1321



July 1989

The Effect of Space Charge on Beams Extracted from the RTECR Ion Source

Z.Q. Xie and T.A. Antaya
National Superconducting Cyclotron Laboratory
Michigan State University
East Lansing, MI 48824-1321

Summary

We have obtained excellent agreement between BEAM_3D [1] calculations and beam profile and emittance measurements of the total extracted beam from the RTECR [2], when a low degree of beam neutralization is assumed in the calculations, as will be presented in this paper. The beam envelope has approximately a quadratic dependence on drift distance, and space charge effects dominate the early beam formation and beamline optics matching process.

In these studies we have used helium plasmas, tuned to maximize the helium 1+, so that the source output was essentially mono-ionic. The RTECR helium 1+ output can be varied from 0.04 - 1.5 milliamps with only slight adjustment of this tune, without producing significant 2+. With this simple He¹⁺ beam extraction over a broad range of intensities, the effect of space charge on the beam formation and matching is much clearer than when multiple species are extracted, aiding analysis, while the results are still be applicable to the more general multiply-charged ion ECRIS extraction.

1. Introduction

Most ECRIS have been built for multiply-charged positive ion injection into accelerators. These sources and injection lines generally must operate over a broad range of charges and intensities. The injection rigidity is generally set by accelerator characteristics. The pressure in

the coupling line between ECR and accelerator is low because the ECRIS main stage pressure is low, and it is desired not to have the beamline constitute a source of gas for main stage operation. The specifications for the beam transport elements are generally obtained by assuming (or extrapolating from existing data) a starting emittance at the source extraction aperture, and tracking that emittance with transport optics codes up to a matching condition near the accelerator. The space charge effects on the beam transport optics are either ignored or assumed to be non-important, though space charge effects are often studied during the design of the ion source extraction electrodes.

In an effort to better understand the requirements for matching ECRIS beams to the superconducting cyclotron at NSCL, we have under taken an analysis of the beam formation process on the RTECR, including the interaction of the initial beams with the first elements of the beam transport system.

Initial emittance measurements on analyzed helium and multiply charged argon ion beams indicated rather large divergences [3], and often triangular shaped beams. To understand these measurements, we shifted to measurements on the total extracted beam before analysis, where we could make direct comparisons with the BEAM_3D code. The initial emittance after extraction seems to be determined by the magnetic contribution to the canonical momentum [4], while the divergence is set by the level of un-neutralized space charge. Control of this divergence is critical to correct matching of ECR beams to beam transport systems.

2. He¹⁺ Beam Technique

We have found that helium plasmas, tuned to maximize the helium 1+, provide good beams for studying the beam formation process in the RTECR. There seems to be a large enough difference in source conditions for helium 2+, that the source can be adjusted such that the total extracted current is at least 90-95% helium 1+, as shown in the spectrum in Fig. 1. Other species do not work as well, for example, H₂⁺ and H⁺ production are more closely coupled in ECRIS, and any heavier mass species will of course have a distribution of extracted charges. The RTECR has a wide dynamic range of helium 1+ production - from a few microamps to milliamps, at low microwave power and essentially constant magnetic field. The required

He Spectrum, $V_{ex} = 10$ KV, $V_p = 0$, RF = 80 Watts

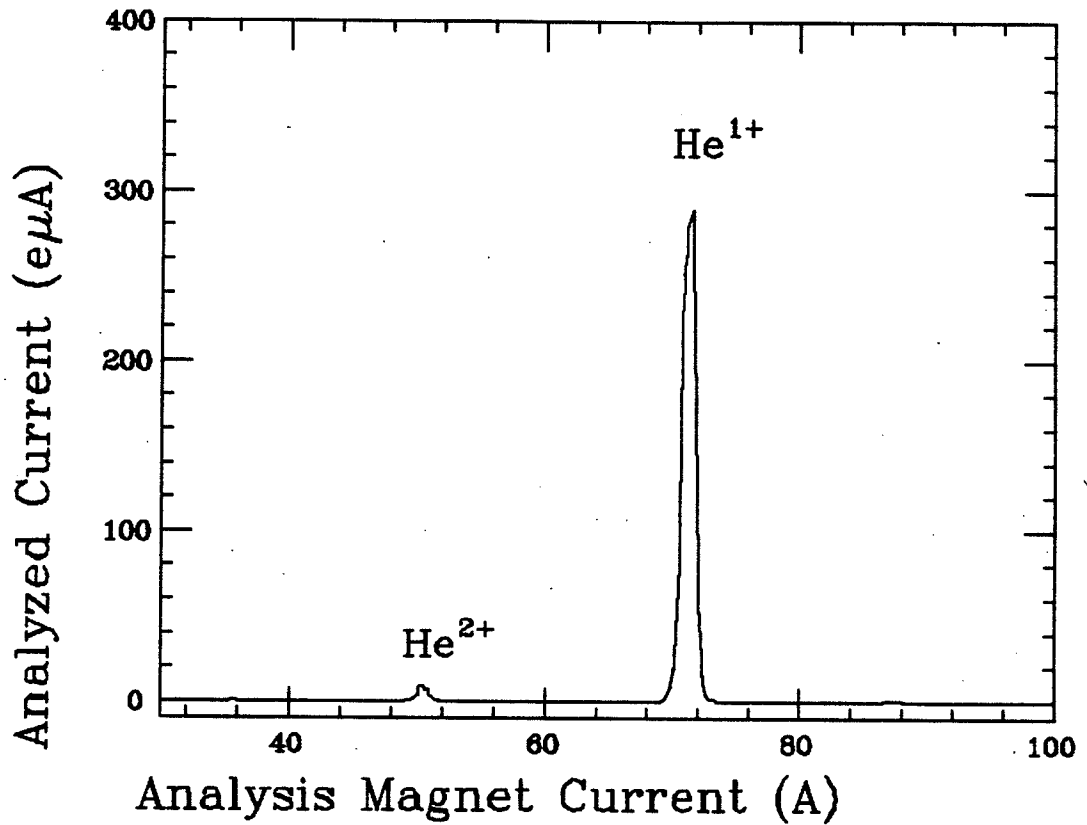


Fig. 1. A helium spectrum is shown here. 300 eμA helium 1+ was produced by the RTECR source at $V_{ex} = 10$ kV, $V_p = 0$ and 80 watts RF power, while less than 5% helium 2+ was produced.

microwave power is ≤ 100 watts, while we typically use 1.2 kW for high charge argon ion production. We expect low thermal energies at such low input powers [5], further simplifying the beam formation process, but the main value of using these helium 1+ plasma is that the extraction gaps and voltages are uniquely determined as a function of space charge for single charged species extraction.

3. BEAM_3D Code

The computer code BEAM_3D is used to study the RTECR beam extraction and pre-analysis beam transport. BEAM_3D is a full 3D extraction code, that includes source electric and magnetic fields (including the hexapole magnet), with simultaneous multiply-charged ion extraction from user defined starting conditions. However, the full features of BEAM_3D have not been utilized in the studies to be reported here. We have found that a reduced problem definition is very adequate for matching experimental helium 1+ measurements. In this reduced problem we do not include the hexapole magnet field, but we have added the first beamline focussing solenoid magnet, and therefore can calculate the vertical segment shown in Fig. 2. Ions are assumed emitting from a plane perpendicular to the optic axis, and the current density of each ion species is assumed to be uniform over the extraction aperture. Ion thermal energy is assumed to be a uniform distribution up to a maximum value specified by input. The space charge force of multiple ion species is handled by summing up the contributions from all the ion species enclosed by a circle of radius r [6]. Following the beam with space charge through the focussing solenoid to the entrance of the analysis magnet is very essential, as will be seen in later discussions, for matching the source conditions to the beam transport system.

4. RTECR Beam Analysis System

The beam analysis system for the RTECR is shown in Fig. 2. The source axis is vertical, with accel-decel extraction at the bottom. The first acceleration gap is adjustable from zero to 3.3 cm. The source extraction aperture is placed at the object of a solenoid focussing lens, which takes the initial beam to the object of the 90 degree dipole magnet (at faraday cup #1), with unit magnification. The solenoid focal length was chosen to

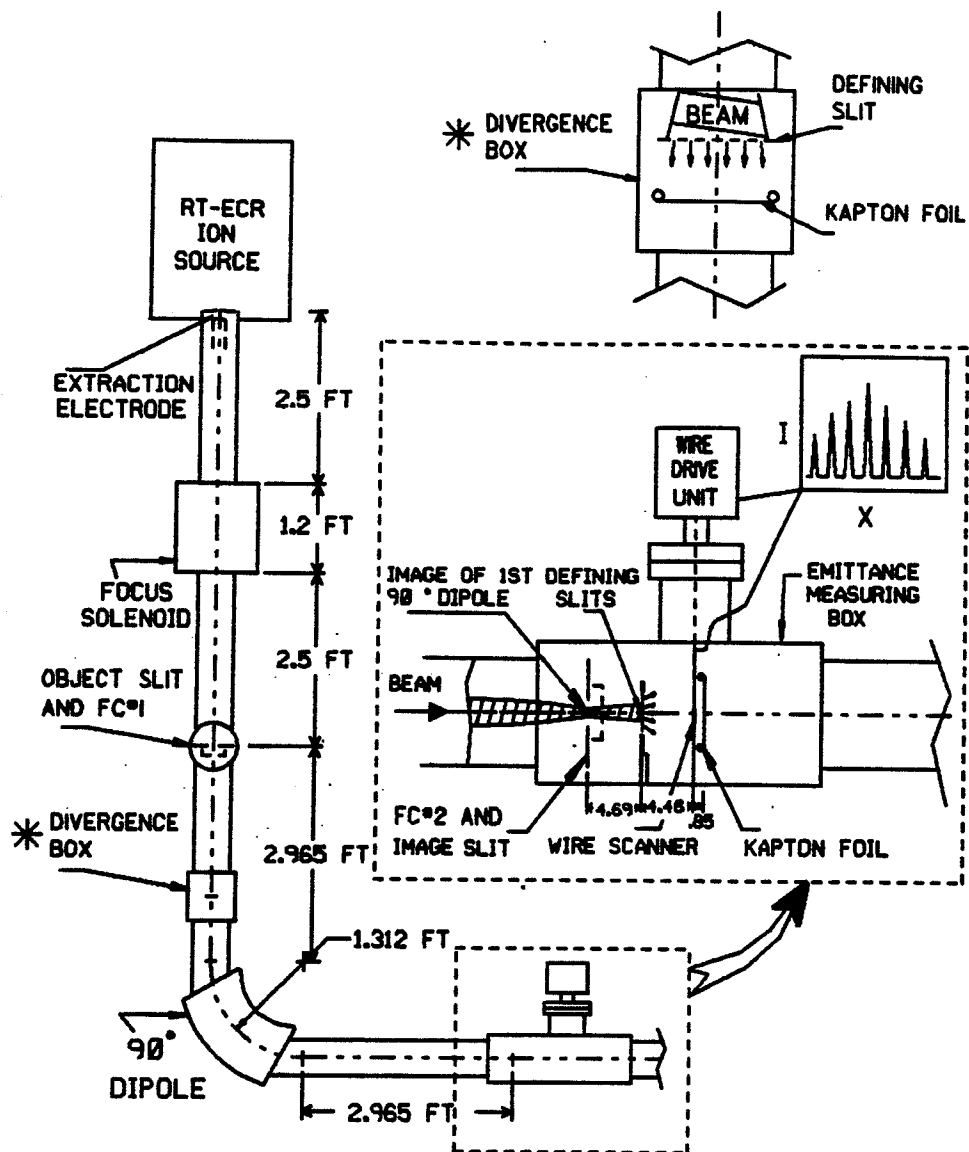


Fig. 2. A schematic view of the RTECR analysis system. Emittance and beam profile measurements can be made at the divergence box and after the analysis magnet.

put the ion source on the experimental hall main floor level, and also to allow Ar^{1+} ions to be focussed at a source bias of 10 kV. Both criteria tend to lengthen the solenoid focal lengths. The double focussing dipole images the beam with unit magnification at faraday cup #2. The beam pipe and solenoid I.D.'s are 15 cm, while the dipole aperture is 10 cm. An emittance of $5 \times 40 \pi$ mm mrad at the source extraction aperture was assumed in the design of the analysis system. The acceptance of the dipole can be limited by changing adjustable object, divergence and image defining slits. Emittance measurements are possible on both the object and image sides of the 90° dipole. In a vacuum box at a position of high divergence before the 90° entrance, emittance measurements are made by imaging a defining slit pattern on kapton film (which darkens on exposure to the beam, with well defined edges). Several images can be made in this 'kapton camera' before the film is removed for analysis. At $100 \text{ e}\mu\text{A}/\text{cm}^2$ current densities or higher, charging effects on the kapton film start to blur the images. At these current densities, we image the beam onto the metallic side of aluminized kapton film and obtain well defined images on the kapton side. In the FC#2 box, we can make emittance measurements in either transverse plane with an on-line wire scanner, or with kapton film exposures or both. The two methods are complimentary. The wire scanner method allows quick determination of the emittance for a variety of tuning conditions, but obscures the incoherent emittance, while the kapton film method shows incoherent effects, such as relative beam motions and multiple beams.

5. Initial Operation of the RTECR Analysis System

The performance of this analysis system, as described above, is as follows. With a total extracted current of 0.5 - 1.5 emA at 10 kV (various source geometries and tuning conditions), the first acceleration gap optimized at the maximum possible value of 3.3 cm, with zero voltage on the decel (puller) electrode. With an analysis acceptance of about 300π mm mrad, the dipole image was always about twice the object size, and the overall transmission, measured as the ratio of FC#2 peak currents to the net extracted current (bias current - zero plasma drain current), or as $\sum \text{FC\#2} / \sum \text{FC\#1}$, was about 40 - 45%. The cause of this overall low transmission, typical for many ECR sources the second author has tuned,

was not understood.

Early emittance measurements using the wire scanner after the analysis dipole showed very high divergence, which, in addition to the poor transmission from FC#1 to FC#2, we could also not explain. In Fig. 3, we show the wire scanner profile and a 90% intensity emittance contour for Argon 10+ ions extracted from the RTECR. The 100% emittance contour (not shown) has an area of $510 \pi \cdot \text{mm} \cdot \text{mrad}$ (to make this measurement the analysis system acceptance was opened to $820 \pi \cdot \text{mm} \cdot \text{mrad}$ -- possible only because of the large magnet apertures). Both the 90% and 100% emittance contours are much higher than would be expected on the basis of thermal energy or angular momentum considerations. The hard edge emittance ($r^2 B$ term) for this beam would be $80 \pi \cdot \text{mm} \cdot \text{mrad}$. Recent emittance measurements at LBL have also shown such large divergences for highly charged argon ions [7]. In that study, it was shown additionally that a decrease in the extraction aperture from 8 mm to 1 mm substantially reduced the high divergence component of the beam -- an observation that we will come back to later in this report.

6. Space Charge Forces and the RTECR Extraction Electrode Design

The RTECR source has a three-piece electrode system, as shown in Fig. 4. For historical reasons, the original puller electrode in the RTECR had a 45° angle while the first electrode "End Plate", following the Pierce theory [8], is at a 67.5° angle with respect to the optic axis as, shown in Fig. 4A. Such an extraction system with a 45° puller does not work properly when the extracted current is at or below the space charge limited current [9]. It has less focussing strength at the beginning of the extraction, and too much at the end, resulting in a drum shape beam profile in the first gap, see Fig. 5A, and a distortion in the phase area after extraction, results in a large initial emittance, as shown in Fig. 6. BEAM_3D suggests that an exact Pierce spherical puller, shown in Fig. 4B, is better than the 45° puller in ensuring a space charge limited current with a parallel beam profile in the extraction region, as shown in Fig. 5B, and less phase area distortion after extraction, see Fig. 6. Therefore a better matching of the down stream beamline should result (brightness \propto square emittance).

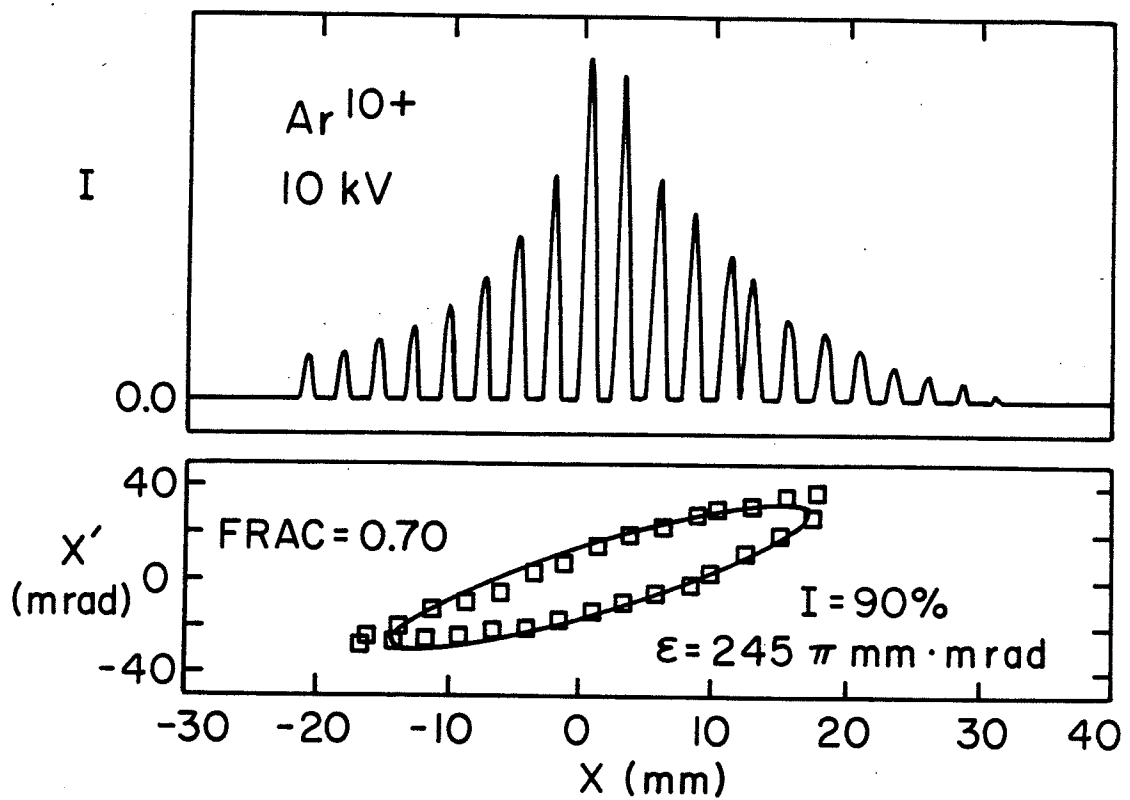


Fig. 3. A 3 μA Ar^{10+} beam profile after the analysis magnet is shown. The large tail is believed due to the high divergence beam component. An ellipse fit at 90% intensity gives emittance $\epsilon = 245 \pi \text{ mm} \cdot \text{mrad}$.

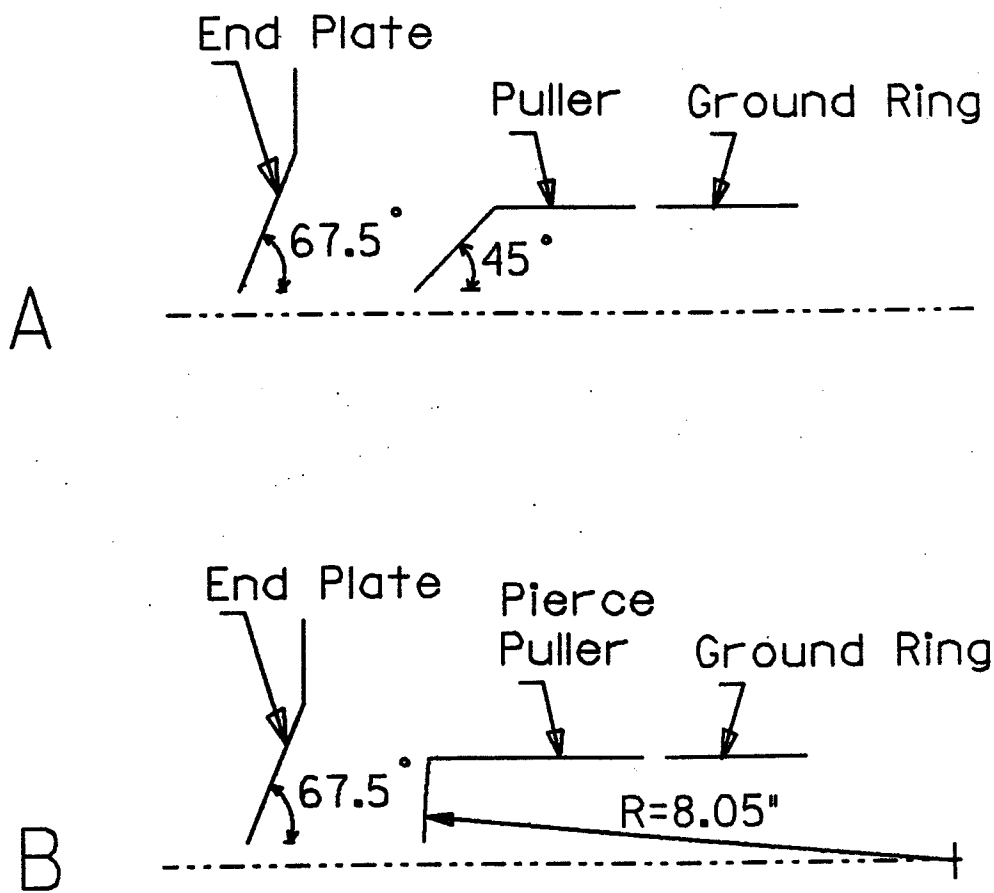


Fig. 4. A schematic view of the two extraction electrode systems utilized in the RTECR. A. The puller has a face angle at 45° . B. The puller has a spherical Pierce face shape [8].

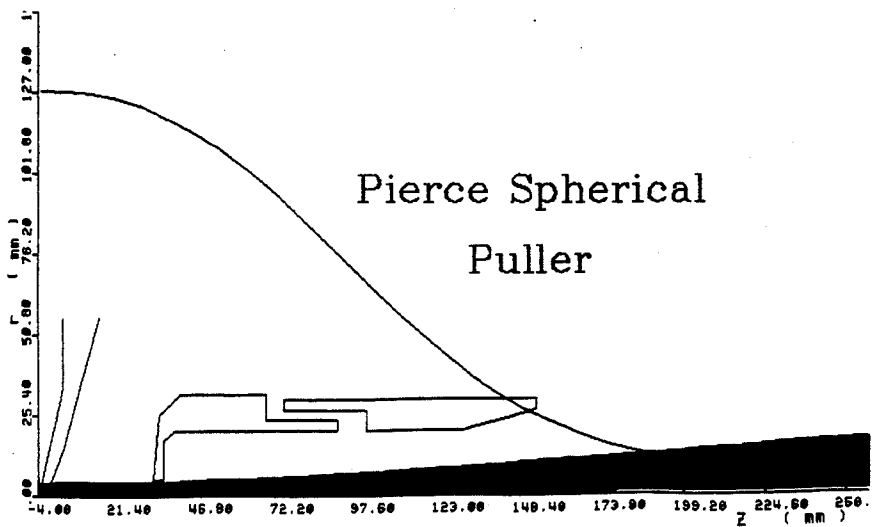
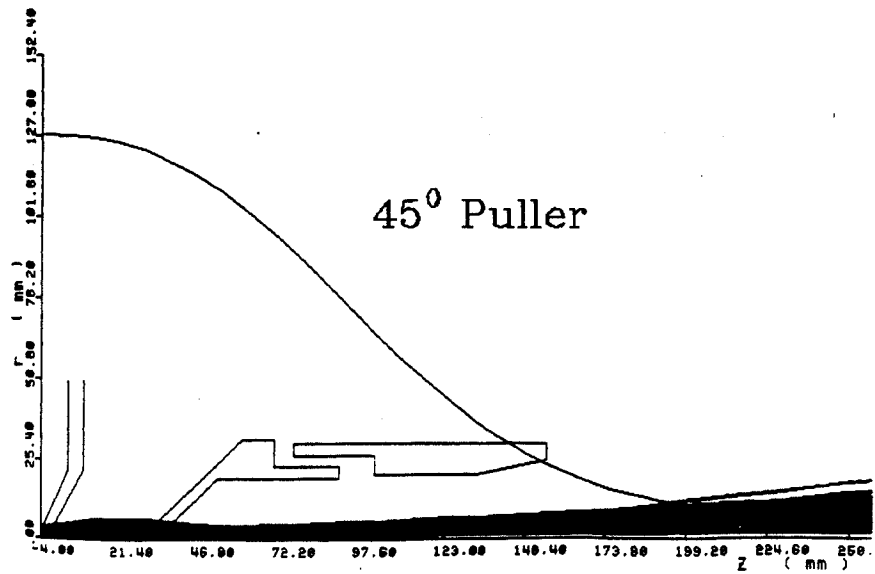
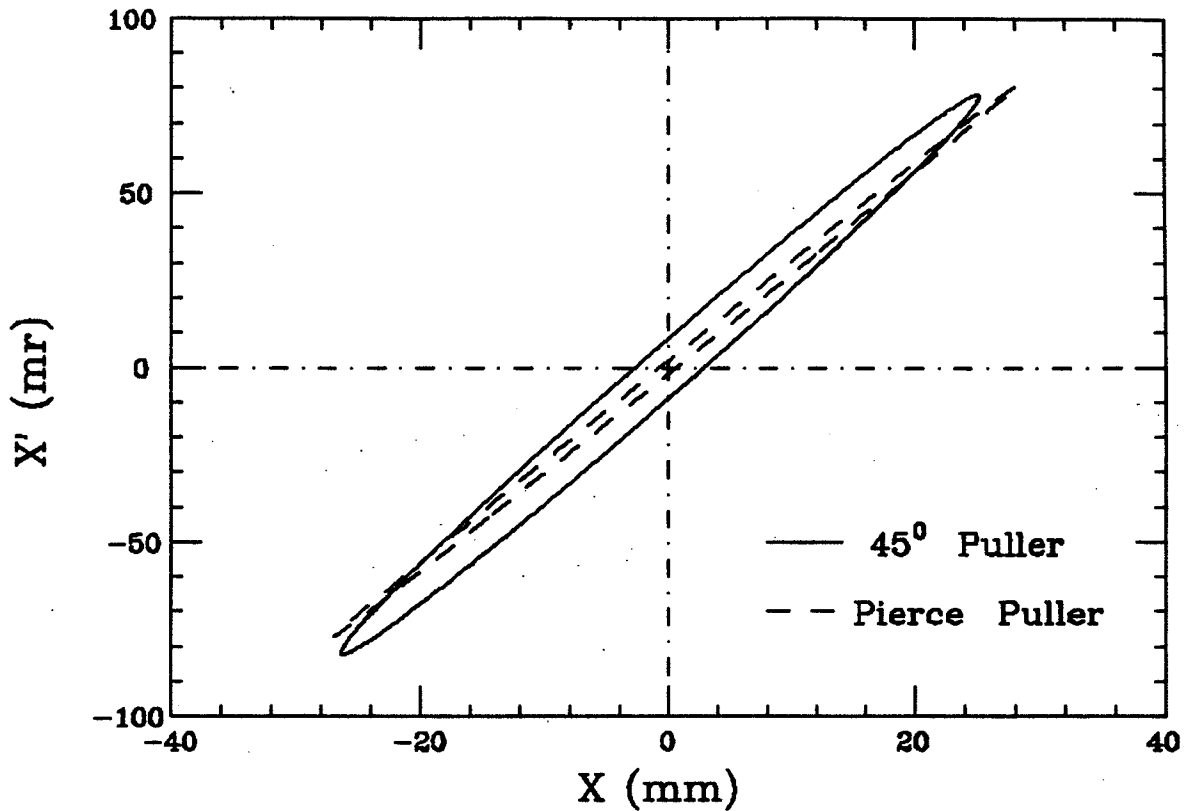


Fig. 5. BEAM_3D calculated beam profiles at a space charge limited current for the extraction system with 45° angle of the puller and a spherical Pierce puller. A drum shape in the first gap, and a focus in the puller electrode are seen for 45° puller of Fig. 4A.

BEAM_3D Cal. He¹⁺, Vex=10 kV, I=1.284 emA



$\phi = 8 \text{ mm}$, $T_{t0} = 0$, $D = 3.3 \text{ cm}$, $Z = 41 \text{ cm}$

Fig. 6. A comparison of the effective emittance after extraction for the 45° and a spherical pullers in RTECR, for a space charge limited He¹⁺ beam of 1.3 emA at D=3.3 cm, with Vex=10 kV. BEAM_3D predicts the effective emittance of the 45° puller is about three times that of the spherical Pierce puller.

Having demonstrated that theoretically that a Pierce geometry is better (smaller initial emittance), two qualifications that must be noted. The first concerns the adjustment of the Pierce geometry. Fig. 7 shows the dependence of total current extracted from the RTECR, for 3 different main stage operating pressures [10]. For these measurements, the source aperture was 8 mm, the extraction gap was 3.3 cm and the puller voltage was zero. The total extracted current is seen to follow the Child-Langmuir limit (labelled theory) up to a saturation voltage, and the saturation voltage is seen to increase with main stage pressure. Along the line labelled $D=3.3$ cm, a parallel beam will be produced in a transit of the first gap (as in Fig. 5B). To the right of this line, a gap of 3.3 cm will result in excess focussing in first gap and therefore higher divergence after extraction.

In match ECRIS beams to accelerators, the source tune is set by the ion production requirements, and the extraction voltage is set by the injection rigidity. So for example, we might find it necessary to operate the source on the lower pressure current curve of Fig. 7 at a net extraction voltage of 10 kV. In that case, to minimize the divergence after extraction, we must decrease the electric field strength in the first gap, by increasing the gap ($D=5$ cm line) or reducing voltage ($\Delta V_p=5$ kV).

To do this properly, one should know when the extracted current is space charge limited. This can be achieved operationally by making the gap and puller voltage tuning parameters. For RTECR injection into the cyclotrons at NSCL, we have in fact generally operated to the right of the $D=3.3$ cm line. Since this was the maximum design gap, the least over focussing would occur at $V_p=0$ ($V_p>0$ was not a possibility), which is exactly how the system did operate (see section 3). Once we realized this limit, the first gap was modified to work from 3 to 7 cm.

The second observation concerns the emittance after extraction in a Pierce geometry for high but still space charge limited currents. Even if a parallel beam is obtained in a Pierce - 1st extraction gap, the divergence after transit of the extraction electrodes will increase with increasing intensity. In Fig. 8, BEAM_3D emittance calculations for helium 1+ beams are compared for these different intensities; in all 3 cases the first gap $D=5$ cm; $V_{ex}(\text{end plate})=10$ kV and the voltage on the puller is

FC#1 Current vs Extraction Voltage

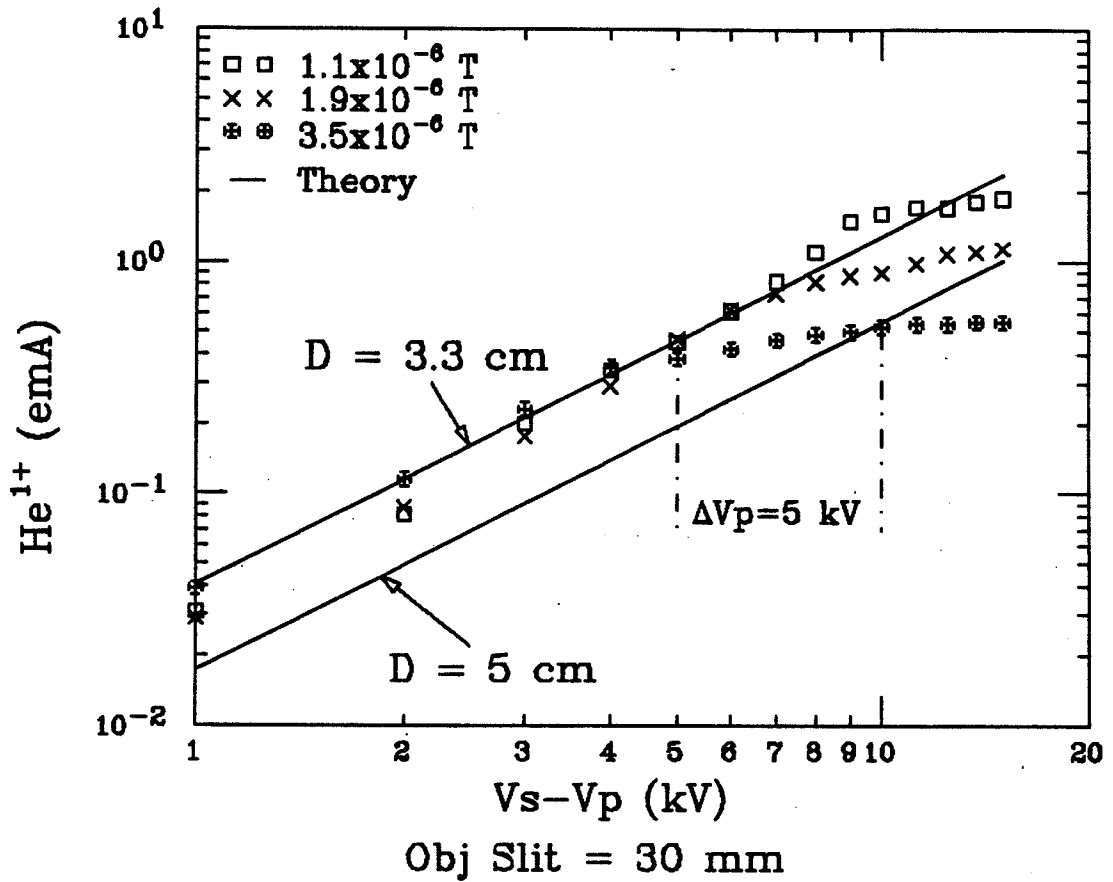
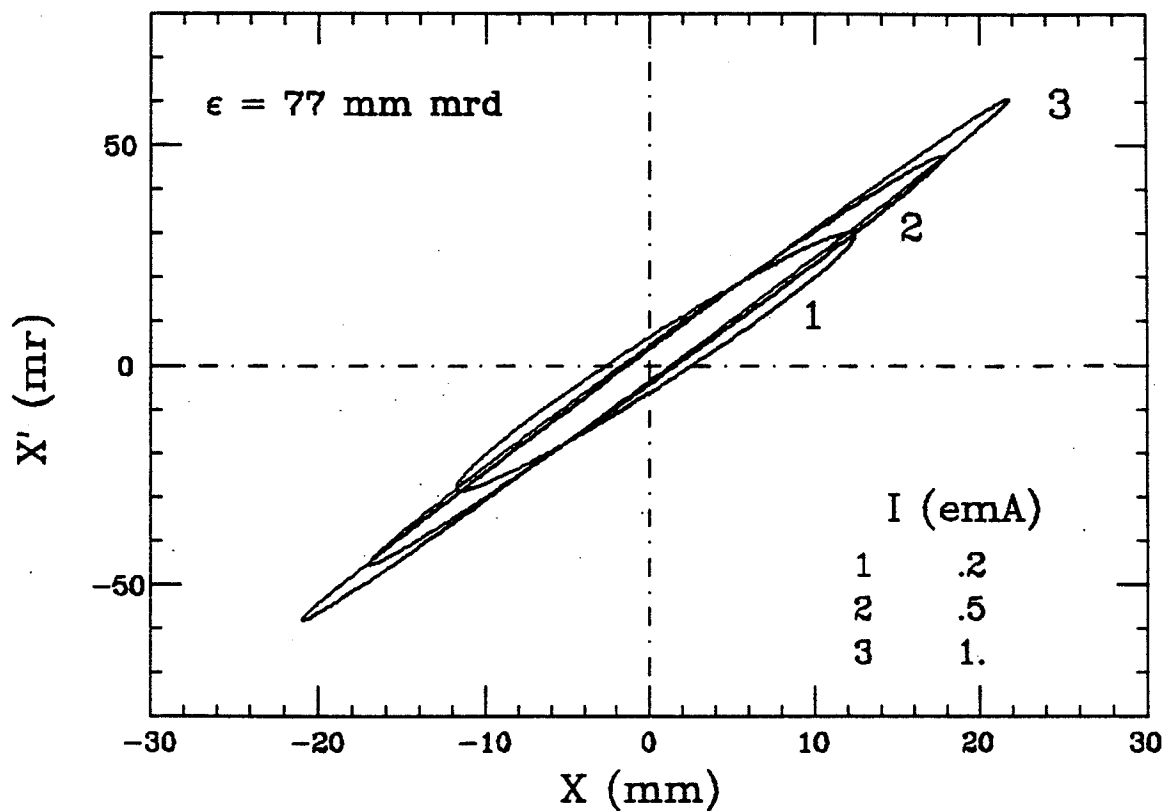


Fig. 7. Using the He¹⁺ technique, the total extracted current of the RTECR was measured directly at FC#1 as a function of extraction voltage, for 3 operating pressures. At low voltages, the extracted current is space charge limited, following the Child-Langmuir law (Theory). At higher voltages the extracted current is seen to saturate.

BEAM_3D Cal. He¹⁺, Vex=10 kV, SCL Currents



$\phi = 8 \text{ mm}, T_{t0} = 0, D = 5 \text{ cm}, Z = 41 \text{ cm}$

Fig. 8. A comparison of the divergence versus beam intensity for space charge limited extraction using the BEAM_3D code. Even though a parallel beam profile at the first gap is ensured, the effect of space charge which increases the divergence is clearly seen.

varied to ensure a space charge limited current in the first gap. The starting thermal energy is taken to be zero. In each case the emittance after extraction is $77 \pi \cdot \text{mm} \cdot \text{mrad}$, but the divergence increases with increasing intensity as a result of the radial space charge force. This is a pure space charge effect -- mitigated only if there is some degree of neutralization in the initial beam. While the 1 emA case in Fig. 8 is typical for the total extracted current from ECR sources, we will show that a significant emittance growth may occur in the transit of the focussing solenoid from such high initial divergences.

7. Initial Observations Supporting Zero Compensation of the Extracted Ion Beam

We have strong evidence that the degree of neutralization in beams extracted from the RTECR is low -- less than ten percent approximately. An early test of the BEAM_3D code was to compare calculated and actual required excitations in the solenoid magnet as a function of space charge ($I=0.1-0.5$ emA) for well focussed He^{1+} beams at FC#1. Since the space force is radial for a cylindrical beam, one would expect the solenoid current to increase with intensity over the base current determined by the ion rigidity, if charge and voltage are held constant. BEAM_3D did predict accurately the required focussing magnet current, if we took for the total extracted current 1/2 of the sum of currents on FC#1 and its defining slits, as shown in Fig. 9 [11]. Since the source was tuned for essentially only He^{1+} output, this result could suggest a 50% loss of beam before FC#1. However, the calculation suggested that even at the highest intensities, all of the $1+$ current should survive to FC#1 -- the beam envelope should stay well within the beam pipe and the spot size at FC#1 should be less than 10 mm. While most of the measured current could be focussed through a 10 mm slit to FC#1, some current was in fact measured on the defining slits before FC#1. The measured ratio of slit current to faraday cup was found equal to the ratio of $\text{He}^{2+}/\text{He}^{1+}$ extracted from the source -- about 5%. (BEAM_3D calculations showed that He^{2+} extracted from the source would be over focussed at FC#1 if the solenoid was set for a correct focus of He^{1+}). A 50% beam loss traversing the solenoid was unlikely, yet excellent agreement with calculated solenoid excitations was obtained using 1/2 the net current on FC#1. One could therefore hypothesis

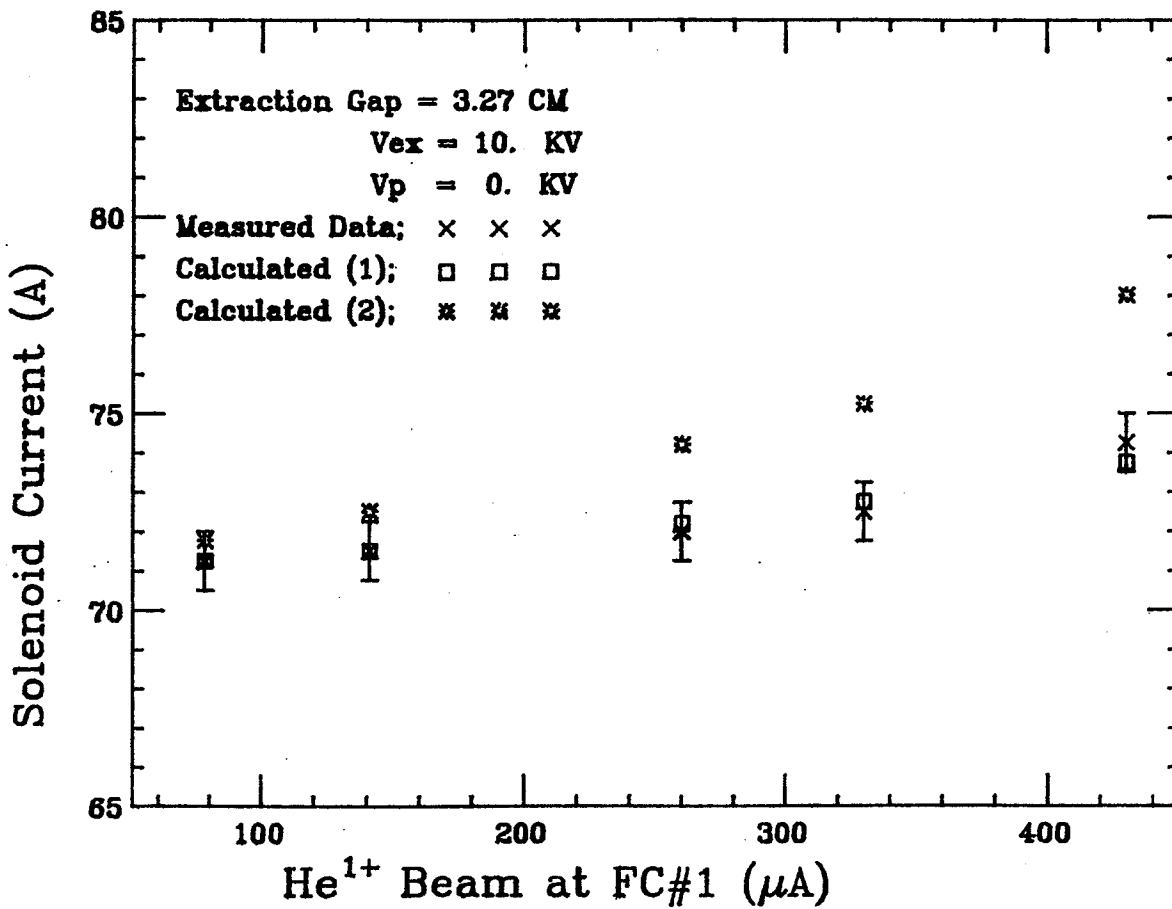


Fig. 9. The comparison between the measured solenoid focussing current for maximum helium 1+ transmission to FC#1 and two calculations, (1) with 1/2 of and (2) with the full sum current on FC#1 and 4 jaw collimators. The extraction conditions were a gap of 3.3 cm, Vex= 10 kV and Vp= 0. The 1/2 sum current calculation gives better agreement, suggesting approximately 50% neutralization, but we later found that about half the measured current was due to secondary electrons generated when beam was stopped on the faraday cup.

a 50% neutralization of the initial beam, since no neutralization was assumed in the calculations, and we made such a hypothesis for these results at the 1987 ECR conference. We have since found however that the positive ion current measured at FC#1 is only 55% of the observed current, the rest being secondary electrons generated when the ions hit the beam defining slits and FC#1. After proper suppression of these secondaries, we find that BEAM_3D correctly predicts the required excitation of the solenoid for a focus at FC#1 as a function of space charge, for the observed total current, assuming zero neutralization.

8. Effect of Zero Compensation on the Initial Beam Transport

The extracted currents in RTECR are in the range of milliamps while the extraction voltages are of a few tens of kV (nonrelativistic motion). Thus the space charge force is not negligible, although it does not increase the beam phase area [12]. To estimate the consequences of the full space charge on the beam transport, we have developed a simple model to show the effect that the space charge has on the envelope of a beam drifting in a field free region, which we will now describe.

The space charge force of a rotationally symmetric beam of multiple ion species is of the form [13]

$$E_r = \frac{1}{2\pi\epsilon_0 r} \sum \frac{I_i}{v_{zi}} \quad (1)$$

where r is the field point, and I_i and v_{zi} are the current and velocity in the z -direction due to the i -th ion species.

An ion on the outmost surface of a beam consisting of multiple ion species, experiences a radial force, in cylindrical coordinates, of

$$\dot{p}_r = \frac{p_\theta^2}{Mr^3} + \frac{Q}{2\pi\epsilon_0 r} \sum \frac{I_i}{v_{zi}} \quad (2)$$

where p_θ is the mechanical angular momentum, a constant of motion, Q and M are the charge and mass of the ion in question, and r is the radius of the beam. The first term can be shown to originate from the initial canonical angular momentum after extraction from the source, while the second term is the radial space charge force in equation (1). Eq. (2) can be rewritten

as

$$\ddot{r} = \frac{p_{\theta}^2}{M^2 r^3} + \frac{Q}{2\pi M \epsilon_0 r} \left[\frac{I_i}{v_{zi}} \right] \quad (3)$$

Integrating Eq. (3) once with respect to time t gives the radial velocity v_r

$$v_r = \left[\frac{p_{\theta}^2}{M^2} \left(\frac{1}{r_m^2} - \frac{1}{r^2} \right) + \frac{Q}{\pi M \epsilon_0} \ln\left(\frac{r}{r_m}\right) \left[\frac{I_i}{v_{zi}} \right] \right]^{1/2} \quad (4)$$

where r_m is the radius of the beam where $v_r = 0$.

Recalling the angular velocity is $v_{\theta} = \frac{p_{\theta}}{Mr}$, one finds the maximum transverse divergence α_t by dividing $v_t = (v_r^2 + v_{\theta}^2)^{1/2}$ by the axial velocity v_z of the ion in question

$$\alpha_t = \frac{v_t}{v_z} = \left[\frac{p_{\theta}^2}{M^2 v_z^2 r_m^2} + \frac{QI}{\pi M \epsilon_0 v_z^3} \ln\left(\frac{r}{r_m}\right) \left[\frac{I_i}{v_{zi}} \right] \right]^{1/2} \quad (5)$$

Eq. (5) indicates that particles on the beam surface will have a constant maximum transverse velocity, and a constant maximum divergence, if the space charge force is zero. This is precisely the condition that is assumed in beam transport calculations when one omits the space charge force. Otherwise α_t is a function of r , which we will show is a function of the axial drift distance z . Thus α_t will be a function of z , that is, the maximum divergence of the beam changes along the optics axis.

The beam profile is obtained by integrating once more with respect to time

$$\int_{r_m}^r \left[\frac{p_{\theta}^2}{M^2} \left(\frac{1}{r_m^2} - \frac{1}{r^2} \right) + \frac{Q}{\pi M \epsilon_0} \ln\left(\frac{r}{r_m}\right) \left[\frac{I_i}{v_{zi}} \right] \right]^{-1/2} dr = t \quad (6)$$

here $t = \frac{\Delta z}{v_{zi}}$ is simply the time that it takes the i -th ions to travel from r_m to r , assuming $t = 0$ at $r = r_m$. There exists no analytical solution for

the left side of Eq. (6), but a numerical integration techniques can be used to give a reasonable result.

To get a feel for the nature of Eq. (6) we can formulate an approximate solution. Let $r = r_m + X$ and assume X is small (short drift). Then we have

$$\begin{aligned} & \frac{p_\theta^2}{M^2} \left(\frac{1}{r_m^2} - \frac{1}{r^2} \right) + \frac{Q}{\pi M \epsilon_0} \ln\left(\frac{r}{r_m}\right) \sum \frac{I_i}{v_{zi}} \\ & \approx \left[\frac{2p_\theta^2}{M^2 r_m^3} + \frac{Q}{\pi M \epsilon_0 r_m} \sum \frac{I_i}{v_{zi}} \right] X \end{aligned} \quad (7)$$

and Eq. (6) becomes

$$t = \left[\frac{2p_\theta^2}{M^2 r_m^3} + \frac{Q}{\pi M \epsilon_0 r_m} \sum \frac{I_i}{v_{zi}} \right]^{-1/2} \int_0^X dx' / X'^{1/2} \quad (8)$$

Performing the integration and re-arranging terms yields

$$r - r_m = \frac{1}{4} \left[\frac{2p_\theta^2}{M^2 r_m^3} + \frac{Q}{\pi M \epsilon_0 r_m} \sum \frac{I_i}{v_{zi}} \right] \frac{z^2}{v_{zi}^2} \quad (9)$$

The beam envelope is seen to have a quadratic dependence on z , with two terms, one due to the initial momentum of the edge particle and the other arising from the space charge force.

For unneutralized ECRIS beams, we will now show that the second term dominates. We have solved equations (5) and (6) numerically for a helium 1+ beams of various intensities extracted at 10 kV from the source, and plot these results in Fig. 10 and 11. At zero intensity, Fig. 10 shows that the maximum divergence is independent of the drift distance, and Fig. 11 shows that a slow increase in beam radius with drift distance will be observed. As the intensity increases both the maximum divergence and beam envelope radius sharply increase with drift distance. An unneutralized 1.0 emA helium 1+ beam will have an envelope radius 4 times the zero space charge radius after a drift of only 1 M. That is an enormous effect. In

Vex=10 KV, Vp=0 KV, Rm=4. mm, Ra=4. mm, Bz= .251 T, He1+

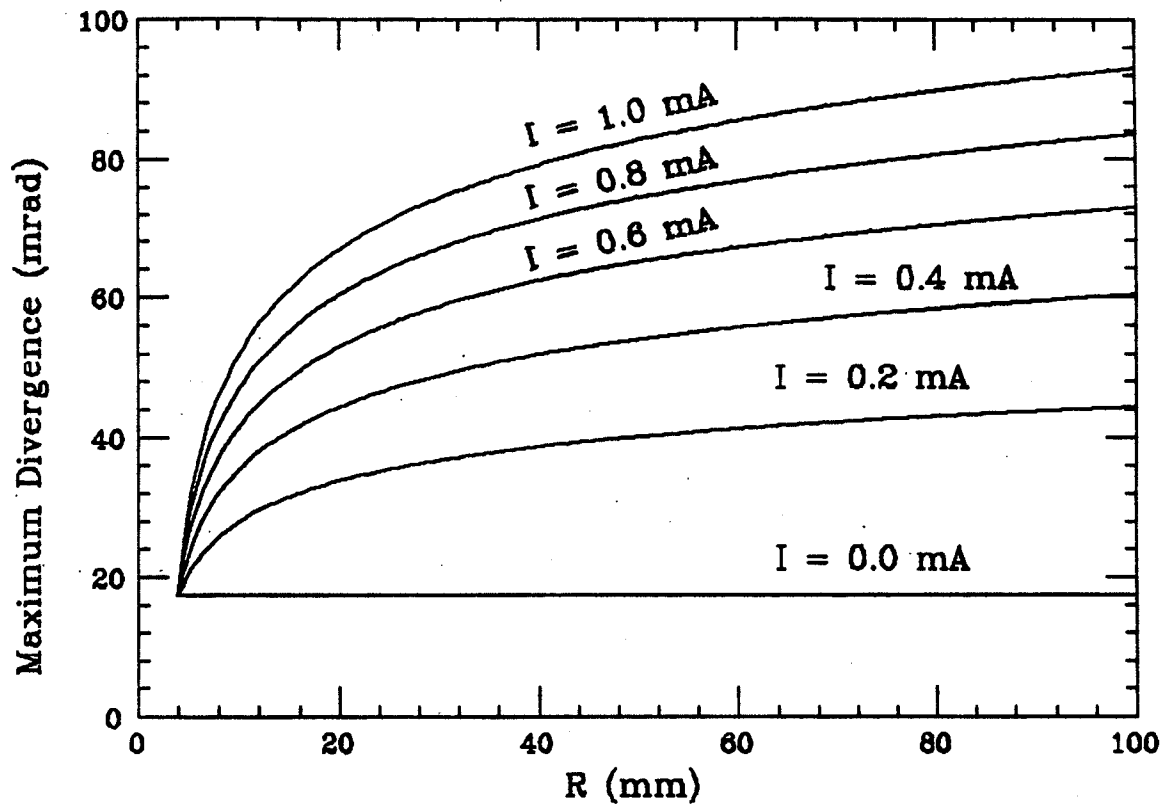


Fig. 10. He¹⁺ beam maximum divergence versus the beam edge radius, for different beam intensities, after a waist. The maximum divergence is a constant if the space charge is zero. But as can be seen, if the space charge force is taken into account, then the beam maximum divergence will increase rapidly with the level of the space charge force.

$V_{ex}=10$ KV, $V_p=0$ KV, $R_m=4.$ mm, $R_a=4.$ mm, $B_z=.251$ T, He $1+$

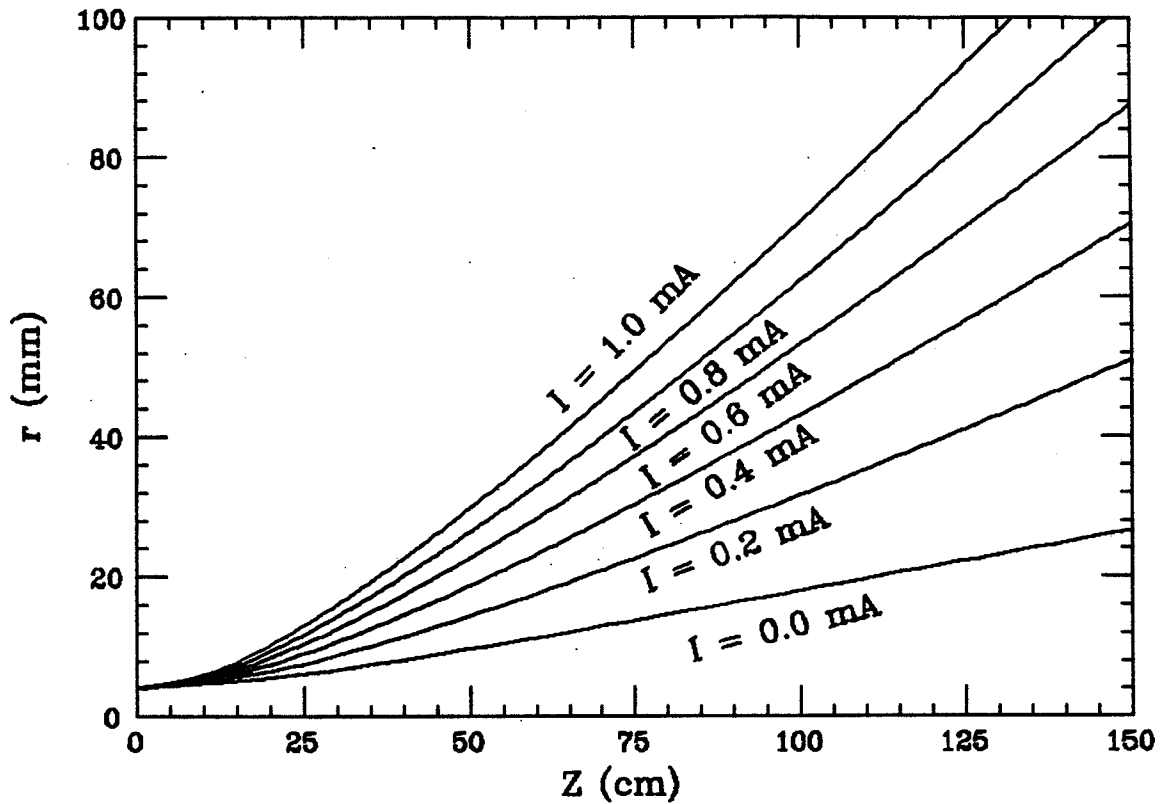


Fig. 11. A comparison of the beam edge radius with axial drift distance for various levels of the space charge. The starting conditions are the same as in Fig. 10. For high uncompensated space charge, the beam envelope rapidly increases with axial drift.

the RTECR analysis system, the distance from extraction electrode to the solenoid center, and the distance from FC#1 to the 90° magnet entrance are both of the order of 1 M.

The RTECR beamline had been designed by assuming a nominal beam emittance ($5 \times 20 \pi \cdot \text{mm} \cdot \text{mrad}$), without taking the space charge force into consideration [14]. But the space charge force is not negligible, at least before the analysis magnet, because we find that the level of neutralization may be quite low. This force increases the maximum beam divergence well beyond the nominal design beam divergence at the entrance of both the solenoid and the analysis magnet, resulting in emittance growth due to lens aberrations. The observed low transmission from FC#1 to FC#2, and the high divergence after analysis, are a consequence of this space charge force. The main point is -- since the divergence grows with drift distance due to this space charge force, the beam transport magnets are not in the right locations to correctly image the beam. This effect is illustrated in Fig. 12. If we examine the emittance of a beam drifting from a waist without space charge, the maximum divergence remains constant and the beam envelope increases. With space charge, the emittance remains constant, but the divergence increases in addition to the beam envelope growth, altering completely the beam transport problem.

9. Space Charge and Transit of the Solenoid Magnet

If the beam crosses the solenoid with a large envelope, there will be an effective emittance growth due to the spherical aberration. This can occur for high intensity ECRIS beams because of low neutralization. Fig. 13 shows the emittance after crossing the solenoid for .065, 0.5 and 1.0 eμA He¹⁺ extracted from the RTECR. In these calculations $T_{10}=0$, so the initial emittance is $69 \pi \cdot \text{mm} \cdot \text{mrad}$ according to the other source conditions. In all three cases the puller voltage is chosen to achieve space charge limited extraction in the first gap. The emittance after crossing the solenoid, plotted at the position of FC#1, are seen to significantly increase with intensity. This is simply due to the increase in the beam envelope due to space charge (as shown in Fig. 11) before the entrance of the solenoid. We have made kapton foil burns in the divergence box for the first two intensities given in Fig. 13, as shown in Fig. 14a for 65 eμA and Fig. 14b for 550 eμA. At the divergence box, one sees a

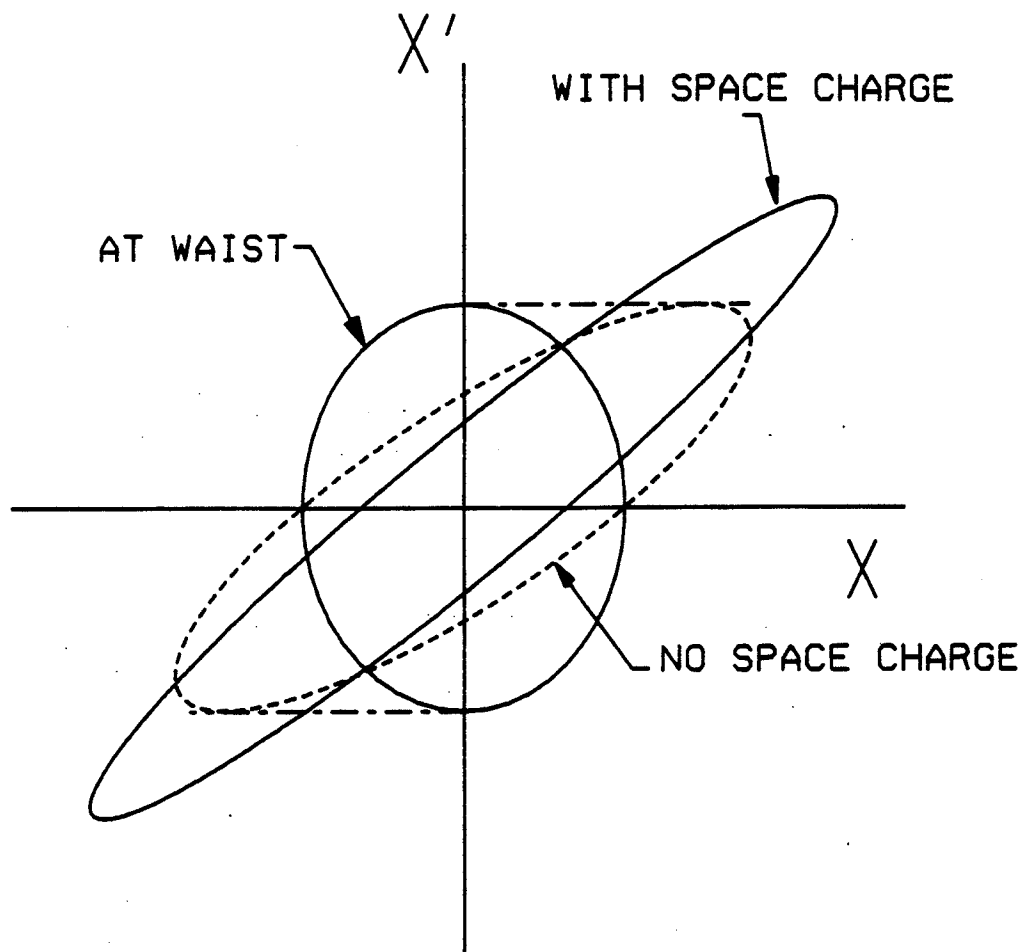
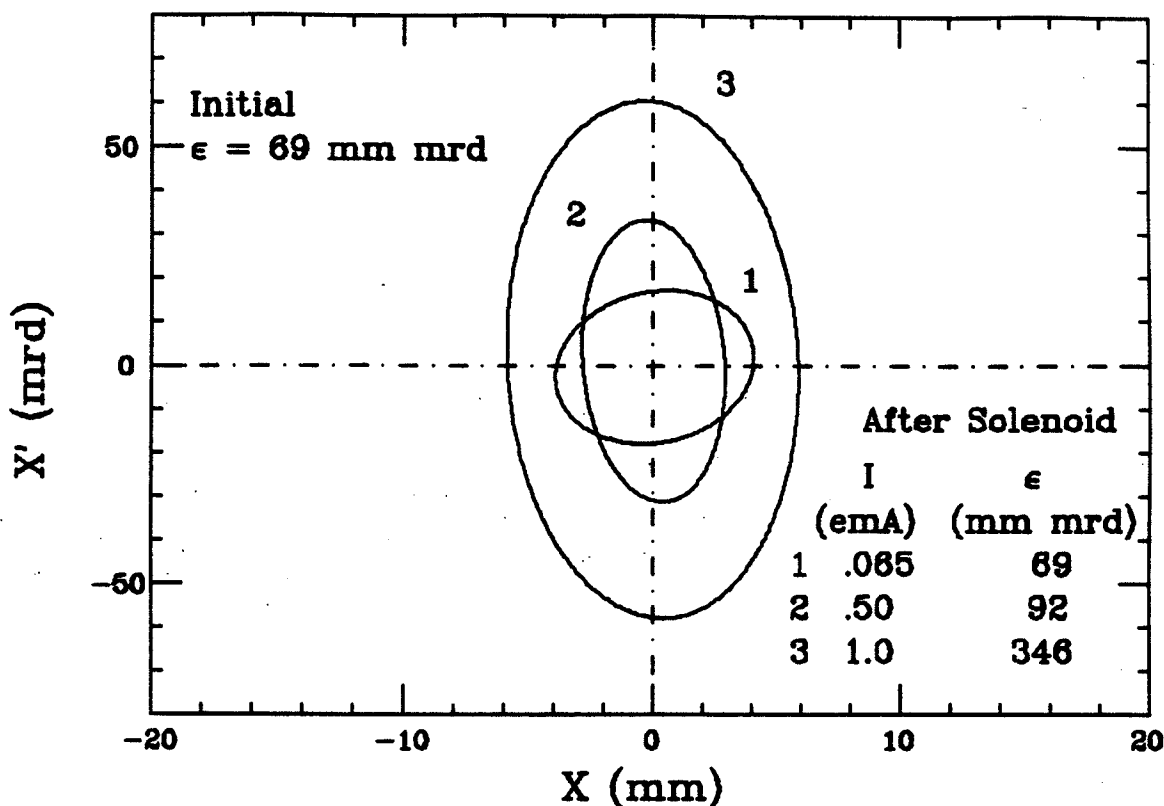


Fig. 12. A schematic view of the evolution of the emittance envelope after a waist with and without space charge force. The emittance are the same for both cases, but with space charge, the maximum divergence and beam size significantly increase.

BEAM_3D Cal. He¹⁺, Vex=10 kV, SCL Currents



$\phi = 8 \text{ mm}$, $T_{t0} = 0$, $D = 3.3 \text{ cm}$, $Z = 190 \text{ cm}$

Fig. 13. The effective emittance of He¹⁺ of various beam intensities after crossing the focussing solenoid. In each case the extraction is space charge limited, the beam energy is of 10 keV, and the emittance after extraction is 69 $\pi \cdot \text{mm} \cdot \text{mrad}$. The 1.0 e mA case shows very large emittance growth due to its large beam profile in the solenoid, thus the aberrations have become very severe.

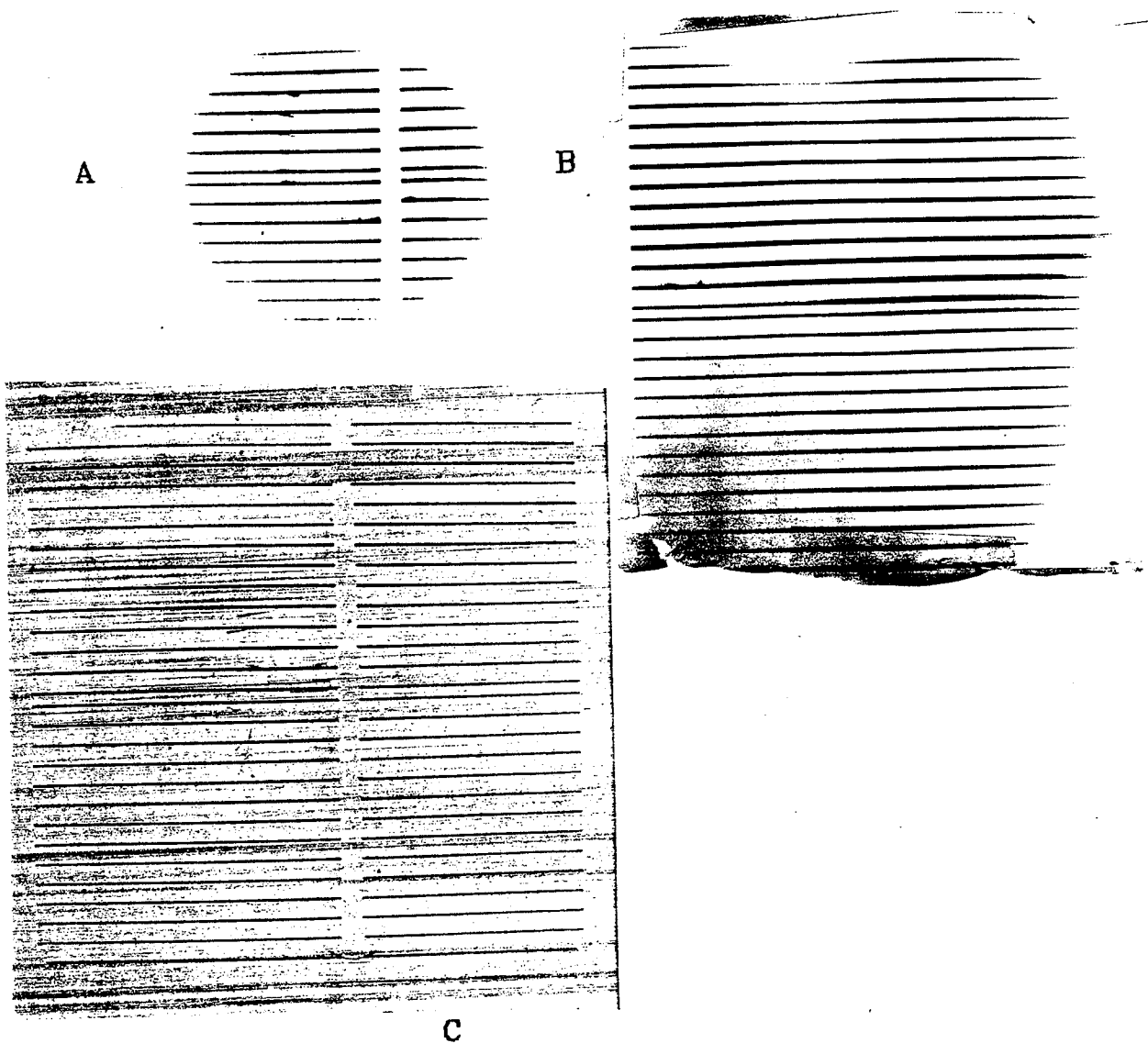


Fig. 14. A, B and C are kapton foil burns at the divergence box with He^{1+} beam of 65, 550 and 65 μA respectively. The beam passes through a defining slit plate 8 cm upstream of the foil, giving horizontal marks on the foil. BEAM_3D predicts for 65 μA He^{1+} at a space charge limit extraction, beam profile at the divergence box will be 1.6" and that is experimentally seen. A 550 μA He^{1+} extracted at space charge limit fills the kapton foil at the divergence box, also agreeing fairly well with BEAM_3D calculation. A 65 μA He^{1+} extracted well below the space charge limited current also results in high divergence and large beam profile at the divergence box.

round image of the source extraction aperture for the 65 μA case (the rectangular patterned in the background is due to He^{2+} over focussed at FC#1, resulting in an image on the foil of the rectangular object defining slit just before FC#1). At 550 μA the beam completely fills the foil aperture. This higher intensity has twice the maximum divergence at the divergence box, according to the foil burns, and this is consistent with the calculation in Fig. 10, taking the 0.70 M distance from FC#1 to the divergence box as the appropriate drift distance.

The corresponding measured emittance at the divergence box for the 65 μA case is shown in Fig. 15. As can be seen, the measured emittance of $69 \pi \cdot \text{mm} \cdot \text{mrad}$ agrees with the calculated starting emittance. In the calculation, with $T_{\perp 0} = 0$ the emittance is determined by the magnetic field. Good agreement with measurement does suggest that the initial emittance of this 65 μA case is dominated by the magnetic field.

If the extracted beam is far below the space charge limit in the extraction gap (voltage greater than space charge limit voltage), the situation is much worse. Fig. 14c shows the same 65 μA He^{1+} beam as in Fig. 14a, but with a higher than required for space charge limited emission electric field in the first gap (corresponding to being to the right of the Theory line in Fig. 7). In that case the beam over-focuses in the extraction gap, giving after extraction a higher divergence for a given emittance, and if this divergence high enough, causes an emittance growth crossing the solenoid, even though the intensity is low. As can be seen, this over focussed 65 μA He^{1+} beam is as large as the 550 μA space charge limited case.

10. Space Charge and Transit of the Analysis Magnet

Because of the unneutralized space charge force, the divergence at the entrance of the analysis magnet can be significantly higher than the assumed in the beam transport design calculations. The transit of the analysis magnet may then result in substantial beam aberrations. We have graphic evidence of this effect for the other operating ECRIS at NSCL, the CPECR. The analysis system for the CPECR differs from that for the RTECR, in that there is no focussing magnet -- the source extraction electrode is placed directly at the object of the 90° magnet (FC#1 in the RTECR system). During the first year of operation of the CPECR, primarily

He¹⁺, 65 eμA at FC#1, Obj. 10 mm, L=7.87 cm

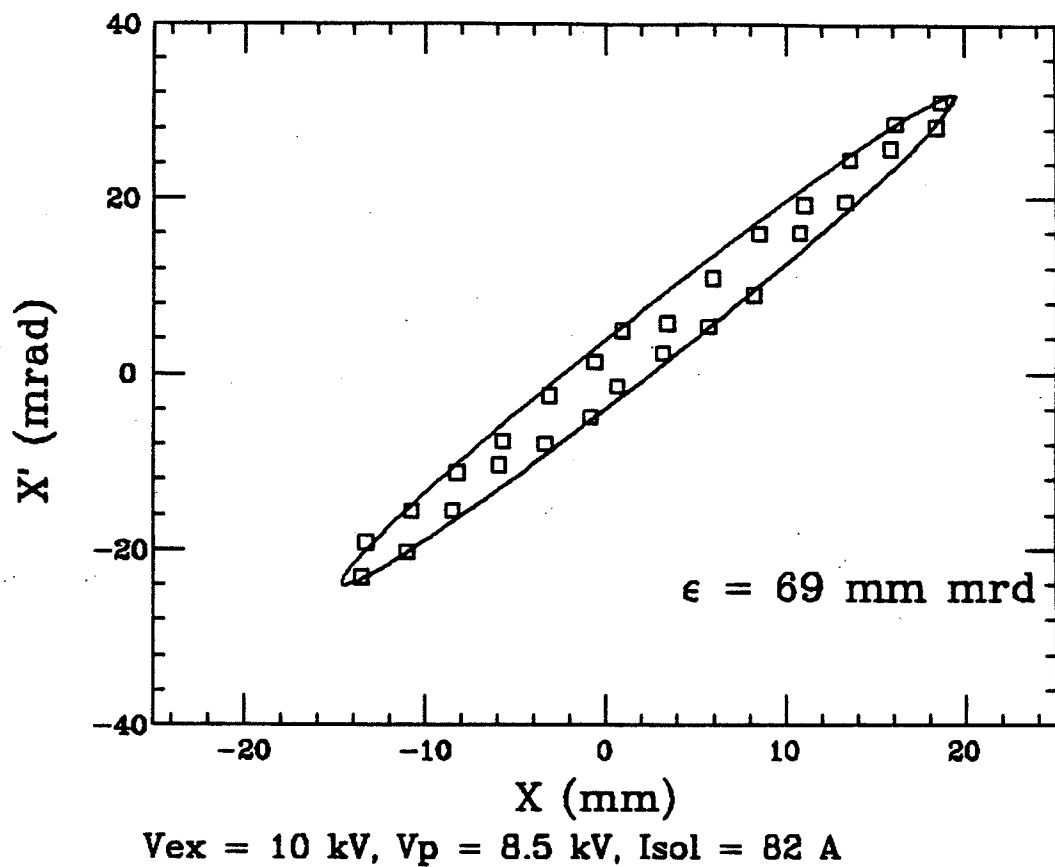


Fig. 15. The measured emittance for the 65 eμA He¹⁺ beam in Fig. 14A is $\epsilon = 69 \pi \cdot \text{mm} \cdot \text{mrad}$, which agrees very well with the BEAM_3D calculation (see Fig. 13), in which the ion thermal energy was taken to be zero.

lithium beams were produced for injection into the k500 cyclotron. For lithium production the source is operated at high pressure on helium support gas with lithium vapor coming from an oven. The total extracted current is about 1 emA with about 50% helium 1+. After about 1 year of operation in this manner the source was moved to a different beamline and the image faraday cup assembly (equivalent to FC#2 in Fig. 2) happened to be removed as a part of this operation. We found a large triangular beam mark on the face of the 4 jaw collimator mounted just before this faraday cup, as shown in Fig. 16.

The bulk of our object side foil burns on the RTECR do not show triangular beams, for example as those shown in Fig. 14, so this mark on the CPECR FC#2 assembly is more likely related to the transit of the analysis magnet than to beam transport calculations at the design emittance (5 mm X 40 mrad) for this dipole design do not show evidence for triangular beams after transit of the analysis magnet [15]. In addition, extensive magnet studies do not show magnetic field errors that might result in triangular beams [16]. If however we consider the transit of the analysis magnet with an unneutralized 1.0 emA beam having the design starting emittance at the object point, we are able to generate the triangular beam marks observed. Fig. 17 shows an intensity contour plot and transverse beam profiles at the image of our dipole magnet with a starting emittance of $200 \pi \cdot \text{mm} \cdot \text{mrad}$ with a 1.0 emA intensity uniformly distributed across the initial beam profile, made using the GIOS beam transport code [17]. The calculated profile has the same shape as the observed spot and is due to second order aberrations resulting from excessive divergence at the magnet entrance. The excessive divergence is due to space charge growth of the initial divergence after extraction. Furthermore, the y-profile in this calculation is strikingly like the scanner profile for Ar^{10+} made after the RTECR analysis magnet that was shown in Fig. 3. In the case of the LBL after analysis emittance measurements mentioned earlier, a reduction of the source aperture from 8 mm to 1 mm cuts both the intensity and initial emittance, so that no significant divergence growth due to space charge would be observed.

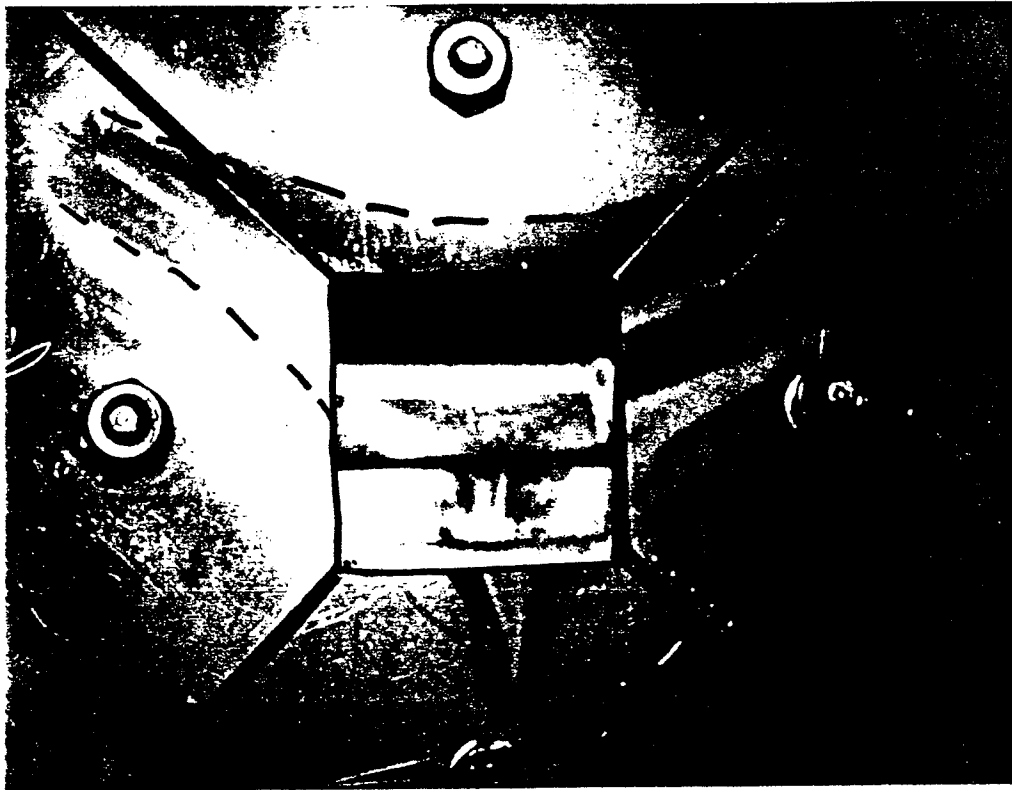
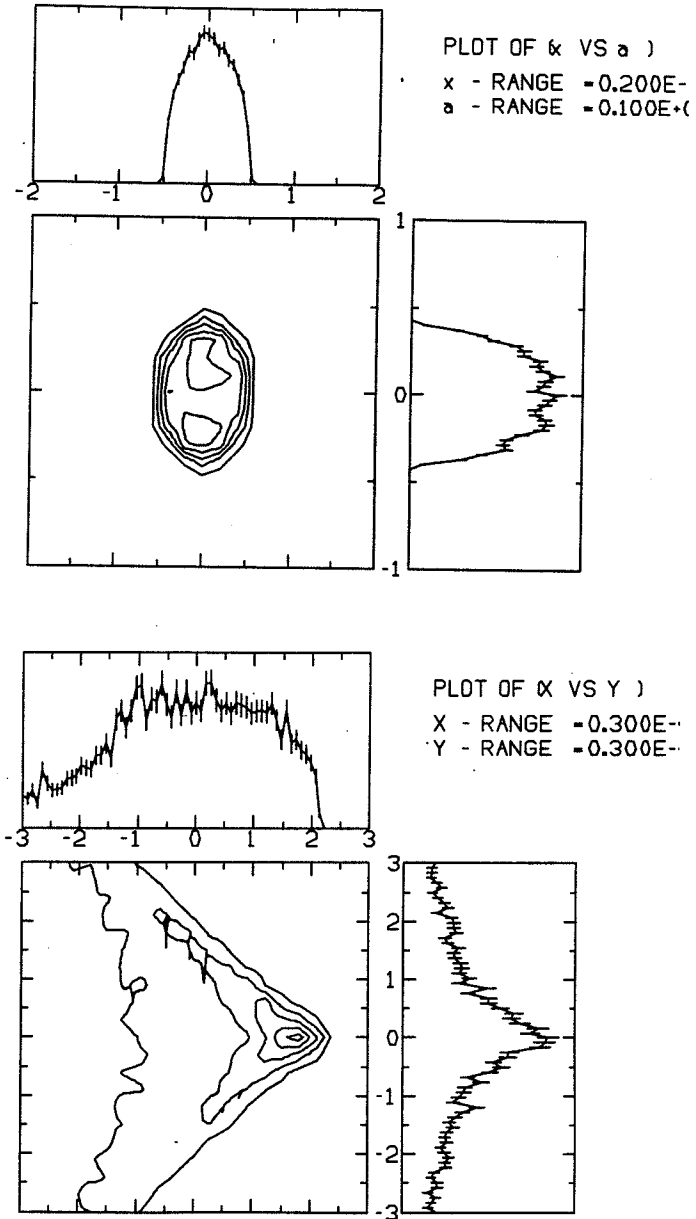


Fig. 16. A triangular beam mark is seen on the face of the collimator of FC#2 assembly for the CPECR. The cause of this triangle shape is believed to be the space charge effect on the beam divergence before the magnet entrance, including 2nd order aberrations.



90 DEGREE MAGNET ;

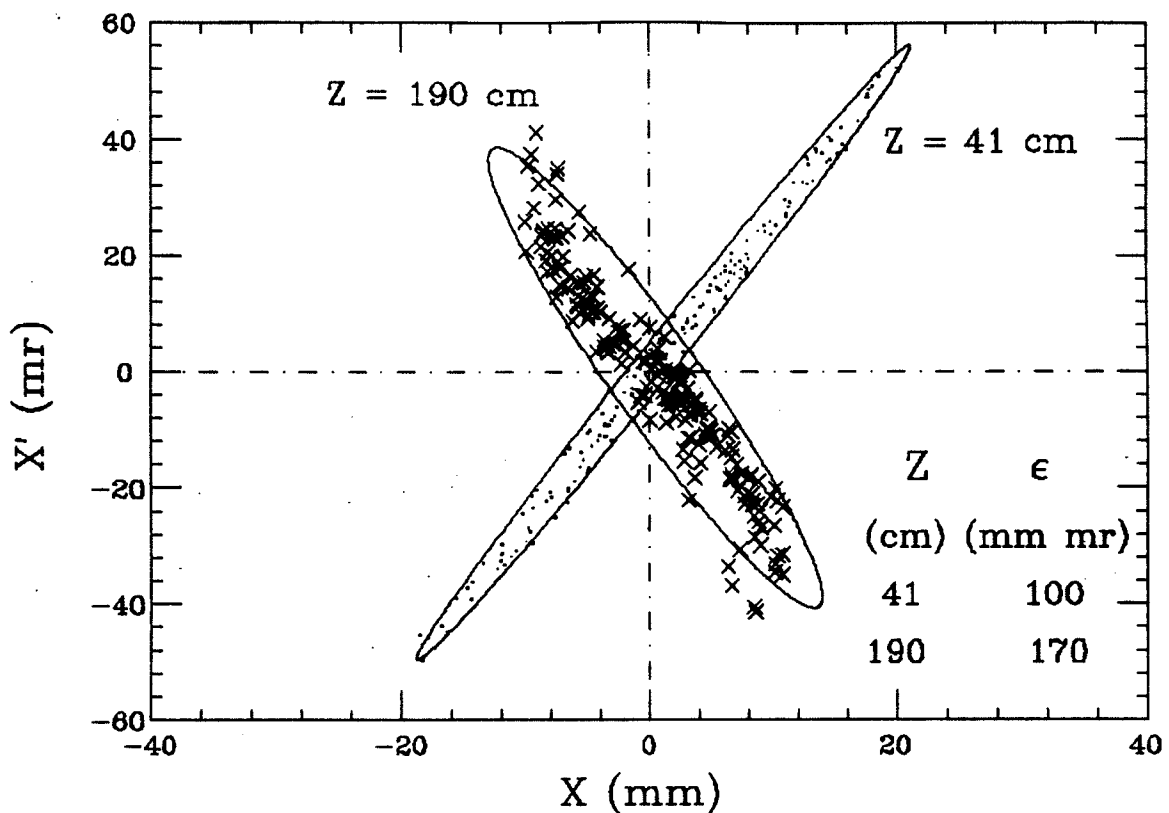
Fig. 17. A GIOS beam transport calculation for the case in Fig. 16. The transit of the analysis magnet with an unneutralized 1.0 emA helium 1+ beam of starting emittance $200 \pi \cdot \text{mm} \cdot \text{mrad}$ will result in a triangular shaped beam after analysis.

11. Extrapolation to Multiply-Charged Ion Extraction from ECRIS

The original motivation for the development of BEAM_3D, and the beam measurements on the RTECR, was to study the emittance and beam transport matching of multiply-charged ions. This has led to the He¹⁺ technique, simplifying both the calculations and the experimental studies. We have found indirect evidence for low neutralization in the initial beam, with several important consequences. It is necessary for the extraction to be space charge limited in the first gap, leading to the use of spherical Pierce lens system, to minimize the initial divergence for any total extracted current. As the intensity is increased, there will be lens aberrations due to substantially larger than design divergence at the magnet entrances. The high divergence tails on ECRIS beams after transit of the analysis magnet is likely due to this effect. Where the beam intensities are high the drift distances between lenses must be shorter than those obtained from zero intensity transport calculations -- the proposed level of operating intensity must be assumed in the design. The good agreement between BEAM_3D and measurements suggests additionally that the plasma boundary and starting thermal energies do not play a significant role in determining the emittance when the source is tuned for these He¹⁺ beams.

The RTECR tunes for multiply-charged ions require much higher microwave power than for the He¹⁺ beams, and gas mixing, and we have measured thermal energies of about 6.5 qeV for higher charged argon ions [18]. As a consequence the starting conditions are likely to be somewhat different for multiply-charged ions than for the He¹⁺ studies reported here. Preliminary calculations for Ar⁸⁺ extraction from the RTECR have been made, using $T_{\perp 0} \leq 5$ qeV, and an actual charge state distribution of intensities among argon ions and oxygen support gas ions. These calculations show that the Ar⁸⁺ ions are sensitive to the full unneutralized beam current before the solenoid entrance. A spherical aberration occurs in the solenoid crossing, increasing the emittance about a factor of two, as shown in Fig. 18. The solenoid does some pre-analysis, but the lost ions are mostly of higher charge than 8+ and do not constitute a significant percentage of the total extracted current. We have then essentially the same problem as for the He¹⁺ beams -- the divergence growth before lenses is a critical limiting phenomenon. We have

BEAM_3D Cal. Ar^{8+} , 16 e μA (FC#2), $V_{\text{ex}}=13.44/-2.18$ kV



$\phi=8/12$ mm, $T_{t0}<5$ qeV, $D=5$ cm, $I(\text{sol})=94.3$ A

Fig. 18. BEAM_3D code predicts that after crossing the focussing solenoid the effective emittance of Ar^{8+} (S shaped, due to the solenoid spherical aberrations) is doubled compared to its effective emittance before the solenoid. The CSD and focussing solenoid excitation are based on actual operating values.

already seen in Fig. 3 that high divergence tails are observed on highly charge argon ions measured after the analysis magnet, and there is an expectation that this will prove to be due to aberrations as a result of high divergence at the analysis magnet entrance, when further measurements are made.

Acknowledgements:

We would like to thank Dr. G. Mank for performing the GIOS calculation shown in Fig. 17.

References:

- 1 Z.Q. Xie and T.A. Antaya, Proc. Int. Conf. on ECR Ion sources, NSCL Report #MSUCP-47, E. Lansing, 1987, p. 420.
- 2 T.A. Antaya, Z.Q. Xie, Proc. 7th Workshop on ECR Ion Sources, Julich, W. Germany, 1986, p. 72.
- 3 T.A. Antaya, Proc. Int. Workshop on ECR Ion Sources, Grenoble, France, 1988.
- 4 O.C. Dermois, Particle Accelerators, Vol. 14, 1983, p. 63.
- 5 Y. Jongen, Proc. 10th Int. Conf. on Cyclotrons and their Appl., IEEE 84CH1996-3, 1984, p. 322.
- 6 Ibid. ref. 1.
- 7 D. Clark, Proc. Int. Conf. on ECR Ion Sources, NSCL Report #MSUCP-47, E. Lansing, Nov 1987, p. 433.
- 8 J. R. Pierce, Theory and Design of Electron Beams, D. VAN NOSTRAND INC., 1954, p. 173.
- 9 Ibid.
- 10 Ibid. ref. 3.
- 11 Ibid. ref. 1.
- 12 R. L. Mills and A. M. Sessler, MURA Rept. No. 433, Midwestern Universities Research Association, Stoughton, Wisconsin, 1958.
- 13 Ibid. ref. 1.
- 14 A.F. Zeller, J.A. Nolen Jr. and L.H. Harwood, NSCL 1985 Annual Report, p. 165.
- 15 J.A. Nolen, S. Tanaka, A. Zeller and N. Bhattachary, Proc. Int. Conf. on ECR Ion Sources, NSCL Report #MSUCP-47, E. Lansing, Nov 1987, p. 454.
- 16 J.A. Nolen, private communication.
- 17 H. Wollnik et al, Nucl. Instrum. nad Meth. A258, 1987, p. 402.
- 18 Ibid. ref. 3.